THE UNIVERSITY OF MICHIGAN RESEARCH INSTITUTE
ANN ARBOR, MICHIGAN

Final Report

MOVING LOADS ON FLOATING ICE SHEETS

James T. Wilson

UMRI Project 2432

AIR FORCE CAMBRIDGE RESEARCH CENTER
AIR RESEARCH AND DEVELOPMENT COMMAND
GEOPHYSICS RESEARCH DIRECTORATE
CONTRACT NO. AF 19(604)-1558
LAURENCE G. HANSCOM FIELD
BEDFORD, MASSACHUSETTS

July 1958

LIST OF FIGURES

ABSTRACT

A simple theory of the coupling between a moving load and the flexural waves generated by it in a floating ice sheet is developed. A number of experiments to verify this theory are reported. These experiments include measurements of the waves resulting from constant-velocity loads and the waves resulting from aircraft landings and take-offs.

The critical velocity for resonance between the moving load and the flexural waves will occur at the minimum wave velocity for flexural waves in the ice sheet. This velocity can be predicted reasonably well from a knowledge of the water depth and the ice properties. For a wide range of ice thickness and water depth, this velocity is in the range of ordinary vehicular velocities.

The experimental data indicate that amplitudes at least three times as great as the "static" deflection can result when a vehicle travels at a velocity corresponding to the minimum wave velocity of flexural waves in the ice.

INTRODUCTION

Dispersive flexural waves are generated in floating ice sheets by moving loads. The theory of such flexural waves was first given by Greenhill[1] and has been elaborated by Ewing and Crary[2] and Press and Ewing.[3] A moving load such as a vehicle or a landing aircraft will generate waves in a floating ice sheet and at some critical velocity, these waves may become considerably larger than the "static" deflection due to the load.

Earlier work on this subject was reported[4] and this report may be considered an extension of that work. A further consideration of the theory of coupling between moving loads and flexural waves has led to a modification of earlier ideas; however, the numerical results reported before are essentially correct.

In the course of the work reported here, two new deflectometers were designed and built and field tests were conducted on sea ice in the bay at Hopedale, Labrador, and on fresh water ice at Garrison Dam, North Dakota. At both Hopedale and Garrison, deflectometer records of aircraft landings and take-offs were obtained.

The tests at Hopedale were conducted by Mr. David E. Willis and the writer. At Garrison, Professor James H. Zumberge, Mr. Donald H. Clements, and Mr. Edwin S. Robinson were members of the field party. The theoretical work was carried out by the writer.

THEORY

FLEXURAL WAVES IN A FLOATING ICE SHEET

The wavelengths of the waves in which we are interested are always long compared with the thickness of the ice. Hence we need consider only the flexural rigidity of the sheet. Further, as the velocities of interest are small compared to the velocity of sound in water, we may consider the water incompressible.

Following Greenhill,[1] we take the x-axis horizontal in the undisturbed water plane and the z-axis positive upward. The equation of motion of the ice sheet is then

$$\rho h \frac{d^2 w}{dt^2} = -D \frac{d^4 w}{dx^4} + p \ , \qquad (1)$$

where

ρ = density of the ice
h = thickness of the sheet,
w = vertical displacement,
D = flexural rigidity of the sheet, and
p = pressure of the water on the ice.

For the water, take the velocity function

$$\phi = A \cosh k(z+H) \cos k\,(x-ct), \tag{2}$$

where

k = 2π/wavelength,
H = water depth, and
c = wave velocity.

This will satisfy the equation of continuity in the water,

$$\frac{\partial^2 \phi}{\partial x^2} + \frac{\partial^2 \phi}{\partial z^2} = 0 ,$$

and the condition at the bottom,

$$\frac{\partial \phi}{\partial z} = 0 \quad \text{at } z = -H.$$

Then, as at $z = 0$

$$\frac{\partial w}{\partial t} = \frac{\partial \phi}{\partial z} \tag{3}$$

$$w = -\frac{1}{c} A \sinh kH \sin k(x-ct) ,$$

and, as

$$\frac{p}{\rho_1} + gw + \frac{\partial \phi}{\partial t} = 0 ,$$

$$p = \frac{\rho_1 g}{c} A \sinh kH \sin k(x-ct)$$

$$- \rho_1 k\, cA \cosh kH \sin k(x-ct), \qquad (4)$$

where

ρ_1 = density of water.

Substituting Eqs. (3) and (4) into (1) gives

$$c^2 = \frac{g/k + \frac{Dk^3}{\rho_1}}{\coth kH + \rho/\rho_1 kh} , \qquad (5)$$

which is Greenhill's result, with the difference in density of ice and water included. This same equation, but with the compressibility of the water accounted for, was obtained by Ewing and Crary.[2]

As

$$D = \frac{Eh^3}{12(1-\sigma^2)} \qquad (6)$$

where

E = Young's modulus and
σ = Poisson's ratio,

we may write Eq. (5) as

$$c^2 = \frac{g/k + \frac{Eh^3k^3}{12\rho_1(1-\sigma^2)}}{\coth kh + \rho/\rho_1 kh} . \qquad (5a)$$

For the cases we are to consider, we can take

$$c^2 \approx \left(g/k + \frac{Dk^3}{\rho_1}\right) \tanh kH, \qquad (7)$$

which compares with

$$c_o^2 = g/k \tanh kH \qquad (8)$$

for waves of open water.

Equations (5) or (7) may be differentiated to obtain the group velocity, C, through the relation

$$C = c + k \frac{dc}{dk} . \tag{9}$$

From Eqs. (7) and (9) we then obtain

$$\frac{C}{c} \approx 1 + \frac{-g/k + 3\frac{Dk^3}{\rho_1}}{2\left(g/k + \frac{Dk^3}{\rho_1}\right)} + \frac{kH}{\sinh 2kH} . \tag{10}$$

Let us examine C and c as functions of k, H, and D. For short wavelengths, c increases rapidly with decreasing wavelength. At large wavelengths,

$$c^2 \approx gH\left(1 - \frac{k^2H^2}{3} + \frac{Dk^4}{\rho_1 g}\right). \tag{11}$$

There will be a minimum for c at

$$k_{c_{min}} = \frac{1}{\gamma}\left[\frac{1 - \frac{2kH}{\sinh 2kH}}{3 + \frac{2kH}{\sinh 2kH}}\right]^{1/4} \tag{12}$$

where

$$\gamma = \left(\frac{D}{\rho_1 g}\right)^{1/4} * \tag{13}$$

As the location of the minimum depends on H, which occurs with k in Eq. (12), we can calculate $k_{c_{min}}$ only in terms of H and γ. Figure 1 gives c_{min} as a function of H/γ. The value of c at the minimum is shown also in Fig. 1.

The group velocity, C, is greater than the wave velocity for wavelengths shorter than that at $c = c_{min}$, less than c for all longer wavelengths, and approaches c at very long wavelengths. Figure 2 is an idealized plot of c and C as functions of λ.

---

*Has dimensions of length and is Assur's[5] "action radius."

MOVING LOAD

For an isolated load on a floating ice sheet, we have from Hertz[6]

$$w = \frac{F}{2\pi\sqrt{\rho_1 g D}} \text{kei}\,(r/\gamma), \tag{14}$$

where

w = the deflection
F = the force on the ice,
r = distance from the load,

and kei is Kelvin's Bessel function of zero order. Figure 3 is a plot of kei (r/γ). From this plot we see that an isolated load produces a "wavelength," λ_w, given by

$$\lambda_w \approx 7.8\gamma \tag{15}$$

or

$$k_w \approx 0.80/\gamma \tag{15a}$$

Let us now consider the waves generated by a moving load. The problem is somewhat different from the classical one of a moving pressure point across still water[7] because a wavelength is prescribed by Eq. (14).

As the load moves across the ice with a velocity, V, waves are generated with wavelengths appropriate to the wave velocity, $c = V$. These waves travel with the appropriate group velocity, C. For $V > c_\infty$ (c_∞ = velocity for infinitely long waves), $C > V$. For $c_{min} < V < c_\infty$, two wavelengths are generated. For the shorter, $C > V$, and for the longer, $C < V$. Hence for $V > c_\infty$, a train of waves precedes the vehicle, and for $c_{min} < V < c_\infty$, there is a train in front and a train behind. The wavelengths of these trains are appropriate [from Eq. (7)] to wave velocities $c = V$.

At $V = c_{min}$, $C = V$ and the waves generated travel with the load.

For $V < c_{min}$, the static deflection shown in Fig. 3 will be propagated but amplified as V approaches c_{min}.

A consideration of the amplitudes leads to a very intractable problem because of the dispersion and the complexity of the response of the ice-water system. It seems clear that the maximum amplitude will occur at $V = c_{min}$*

*In an earlier report[4] it was suggested that c_w would be the critical velocity. This seems unlikely in view of the present discussion, although numerically c_w and c_{min} never differ markedly.

despite the fact that for all values of H/γ, $\lambda_w < \lambda\, c_{min}$ and, in fact, for $H/\gamma < 1$, $\lambda\, c_{min} > 2\lambda_w$.

The case of a moving load on a beam on an elastic foundation has been treated by Kenney.[8] This problem is similar to the one here; however, there are important differences. For $V < c_{min}$, where there are no free waves in either situation, the problems are similar and Kenney's results should apply reasonably well if we consider a moving line instead of point source. For $V > c_{min}$ the two cases are not so similar. In deriving the relations for flexural waves earlier, the dynamic reaction of the water on the ice was, of course, included, but this term does not appear in Kenney's situation, and hence for $V > c_{min}$, his results are not completely applicable. Nonetheless, his solutions should give the main features to be expected in the case at hand.

As Kenney's paper is quite available, his derivation will not be reproduced here. Essentially the method he follows is to write the equation of motion [Eq. (1)] with

$$\frac{d^2w}{dt^2} = V^2 \frac{d^2w}{dx^2}$$

and $p = \rho_1 w$ and solve for w with the wavelength prescribed by the static condition.

For no damping and for $V \leq c_{min}$, he obtains

$$w = w_o \frac{c^{\mp\alpha Kx}}{\alpha}\left(\frac{\pm\alpha}{\beta} \sin \beta Kx + \cos \beta Kx\right), \qquad (16)$$

where

K = 2π/static wavelength
w_o = the static deflection

$$\alpha = \left(1 - \frac{V^2}{c_{min}^2}\right)^{1/2}$$

$$\beta = \left(1 + \frac{V^2}{c_{min}^2}\right)^{1/2},$$

and the upper signs are taken in front of the load (x positive) and the lower signs behind.

For no damping and $V > c_{min}$, he obtains

$$w = w_o \left\{ \frac{-2 \sin K(\beta \pm \alpha') x}{(\alpha' \beta)^{1/2} (\beta \pm \alpha')} \right\} , \qquad (16a)$$

where

$$\alpha' = \left(\frac{V^2}{c_{min}^2} - 1 \right)^{1/2} ,$$

and the signs are taken as before.

It is clear that, at $V = c_{min}$, the amplitude becomes infinite. Kenney also gives solutions for the damped case, but we are not in a position to evaluate the damping. However, on the assumption that the damping is small, we may reduce his solutions at $V = c_{min}$

to $$w = w_o \frac{1}{2^{3/4} \delta^{1/2}} \left(\sin \sqrt{2} Kx + \cos \sqrt{2} Kx \right) , \qquad (16b)$$

where δ = the damping as a ratio of critical, and $\delta << 1$.

From this it is evident that even slight damping will prevent w from enormously exceeding w_o. For example, if δ is as large as 0.1, $w < 3w_o$. The relaxation time of ice may be as small as a few hundred seconds and there will be some damping from the water; thus δ may well be of the order of 0.1.

Figure 4 is redrafted from Kenney (his Fig. 1b) and should be compared with data presented later.

LOAD WITH VARYING VELOCITY

Assume a plane landing at a time $t = 0$ and decelerating such that its velocity is given by

$$V = V_o - at. \qquad (17)$$

If then at a distance x from the point of touchdown V = Vd,

$$V = V_o \qquad (17a)$$

and

$$t_d = \frac{2x_d}{V_o + V_d} \tag{18}$$

Now if the waves from the plane are observed at $x = x_d$, the first waves will arrive at a time $t = x_d/U_o$, where U_o is the group velocity appropriate to V_o. Succeeding waves will arrive at times given by

$$\tau = t + \frac{x_d - V_o t + 1/2\ at^2}{U} , \tag{19}$$

where U is the group velocity appropriate to V as given by Eq. (17).

For $V > c_\infty$, $U > V$ and the waves will precede the plane. As observed at x_d, the waves will lengthen in period as the plane approaches and, further, will increase markedly in amplitude because of the approach to resonance, the nearer approach of the plane, and the increasing load as the plant loses lift.

For $c_{min} < V < c_\infty$, the same condition will exist ahead of the plane, but behind the plane there will be waves corresponding to the wavelength that is appropriate to V but greater than the wavelength at $V = c_{min}$ (see Fig. 2).

On take-offs, the wave pattern is influenced by the fact that the plane is accelerating and gaining lift. In general it will be expected that the plane will be preceded by waves of relatively short wavelength and followed by a train of waves having a wavelength equal to or greater than λc_{min}. Those waves generated at $U \approx c_{min}$ may be the dominant train.

OBSERVATIONS OF COUPLING TO MOVING LOADS

EARLIER WORK

Some results of the coupling between moving loads and flexural waves have been presented earlier.[4]

The most important data were taken at Mille Lacs, Minnesota, in February, 1955. Figure 5 shows displacement records at various speeds of passage of a 6000-lb vehicle. The ice was 2 ft thick over about 10 ft of water.

From Fig. 5 it is evident the maximum amplitude is at a velocity near 15

mph. From Figs. 1 and 2 it can be deduced that if we take

$$\gamma = 1000 \text{ cm} \approx 33 \text{ ft},$$

then

$$c_{min} = 545 \text{ cm/sec} \approx 12 \text{ mph},$$

and

$$\lambda_w = 7800 \text{ cm} \approx 255 \text{ ft},$$

which agrees quite well with the observations. The observed wavelength is about 350 ft, which is greater than λ_w, but $\lambda_{c_{min}}$ will be 1300 ft for the conditions deduced above, and it seems likely that, particularly for $H/\gamma < 1$, the observed wavelength at resonance may be greater than λ_w.

NEW DATA. HOPEDALE, LABRADOR

In February, 1956, a number of tests were conducted on the sea ice in the bay at Hopedale, Labrador. These tests were conducted with the aid and cooperation of the AC and W squadron at Hopedale, commanded by Major John Green, USAF, and personnel of the Snow, Ice, and Permafrost Research Establishment who were conducting tests on the sea ice.

Figure 6 shows records similar to those taken at Mille Lacs. The vehicle used was of the same type and the tests were performed in the same manner but with a different deflectometer. The new deflectometer is shown in Figs. 7 and 8. Its magnification is 5 and its normal chart speed is 2-1/2 in. per minute. The tests shown were made on the landing strip on the bay. Figure 9 is a sketch map of the strip. The slant of the records is due to the tide in the bay.

The records indicate a critical velocity of about 25 mph. The ice was a little over 2 ft thick and the water depth was about 40 ft. As the observed static deflections were about 25% greater than at Mille Lacs for the same load, γ should be about 12% less, or about 900 cm. Then from Figs. 1 and 2,

$$c_{min} = 1070 \text{ cm/sec} \approx 24 \text{ mph}$$

$$\lambda_w = 7000 \text{ cm} \approx 230 \text{ ft}$$

$$\lambda_{c_{min}} = 10{,}700 \text{ cm} \approx 350 \text{ ft}.$$

The agreement is gratifyingly good. It seems probable that the difference in record character as well as the greater amplification observed at Hopedale is due to the fact that with

$$H/\gamma > 1, \ \lambda_w \approx \lambda_{c_{min}}.$$

The damping indicated by the Mille Lacs tests is about $\delta = 0.3$, while that for Hopedale is about $\delta = 0.15$. For $H/\gamma < 1$, a good share of the apparent damping is probably due to the mismatch of the wavelengths while for $H/\gamma > 1$, most of the damping is probably due to viscous losses in the water and ice.

AIRCRAFT LANDINGS AND TAKE-OFFS, HOPEDALE, LABRADOR

In February, 1956, a number of measurements were made on the landing strip on sea ice at Hopedale, Labrador. Two deflectometers (see Figs. 7 and 8) were set up along the landing strip (Fig. 9) and a number of landings and take-offs of C-47 aircraft were recorded. The aircraft operations were not designed specifically for the tests but were done as cooperatively as weather and schedules permitted.

Figure 10 shows several of the records. The difference in size of the two landing records shown is due to a difference in distance from deflectometer to plane track and probably also to differences in load on the ice as a function of lift due to aircraft speed as it passed the deflectometer. All the records taken are very similar to those shown.

Taking the values deduced above in discussing a constant-velocity load on the Hopedale ice, we find

$$\lambda_w/c_{min} \approx 6\text{-}1/2 \text{ sec}$$

$$\lambda_{c_{min}}/c_{min} \approx 10 \text{ sec},$$

which are to be compared with the observed period of 7—8 sec for the largest amplitude wave associated with the landing plane. It should be noted that the waves following the plane also have periods of approximately 10 sec and probably represent waves of length $\lambda_{c_{min}}$.

Figure 11 shows c and C as a function of λ, for $D = 0.6 \times 10^{15}$ dyne cm, $H = 1500$ cm, and $h = 60$ cm ($\gamma = 885$ cm). These values are approximately right for the Hopedale tests. If we take the speed at touchdown of the plane as 75 mph (110 ft/sec), the first waves to arrive from the landing should have a period (from Fig. 11) of 75 ft/110 ft/sec = 0.7 sec. The first periods shown on the landing records in Fig. 10 are certainly of this order, although not well resolved. The general character of the landing records are as deduced theoretically in an earlier section of this report. Considering the variables, an attempt to analyze the records more quantitatively does not appear promising.

To a first approximation, the take-off records show a simple dispersive train starting with short wavelengths. Unfortunately, all the take-offs were observed with the deflectometer too far down the strip from the plane. As a

result, the plane was always in the air several hundred feet before it reached the deflectometer. As the take-off runs were short, the observations at a distance were as if the plane were a variable frequency source fixed in space.

The maximum amplitude in the tail of the take-off records has a period of about 11-1/2 sec, which is close to that expected for the minimum phase velocity.

GARRISON DAM, NORTH DAKOTA

The aircraft tests at Hopedale in 1956 verified tentative predictions made on the basis of the Mille Lacs tests in 1955 but were inconclusive in many respects. Most importantly the deflectometers at Hopedale had to be placed on the edge of the runway as they stood above the ice. Further, the tests were made only with relatively low-speed airplanes (C-47's). Consequently some tests were carried out on the lake behind Garrison Dam, North Dakota, in February, 1957.

For these tests an entirely different deflectometer was designed and built. Figure 12 is a schematic drawing of this instrument. A wire from the ice sheet to the bottom carries an iron core that, by its relative motion with respect to a pair of coils attached to the ice, unbalances an inductance bridge. The unbalance is recorded on a recording millimeter. The deflectometer worked satisfactorily but should be completely redesigned for further use. The problems of inserting it into the ice and adjusting the core position through 2 ft of ice (at air temperatures of -10°F) were solved more by luck than by predesign. The 60-cps current for operation of the bridge was supplied by a vibrator from a 6-volt storage battery. The extremely cold temperatures in which the tests were made reduced the battery voltage and more or less invalidated calibrations made earlier.

A landing area was prepared on the ice by the Garrison District of the Corps of Engineers, U. S. Army. Figure 13 is a sketch map of the landing strip. The tests would have been impossible without the cooperation of the District and the District Colonel, Colonel Lynn M. Pine, USA. The Snow, Ice, and Permafrost Establishment, Corps of Engineers, U. S. Army, were conducting tests at the same time and their party, directed by Mr. G. Frankenstein, was of inestimable aid.

A C-131 aircraft piloted by Lt. Col. Richard D. DeStaffany, USAF, made three landings. After each landing the airplane taxied back over the deflectometer. The ice was about 2 ft thick and the water depth at the deflectometer was about 50 ft. The depth was fairly uniform except for the old river channel near the bluff at the southeast end of the strip.

The aircraft weighed 42,000 lb for the first landing and 41,000 for the third. The touchdown speed for the first and third landings was about 85 knots

and was 92 knots for the second landing. For all landings the plane touched down about 1500 ft before the deflectometer and had slowed to about 40 knots at the deflectometer. For the first and second landings the flaps were retracted to take-off setting as soon as the touchdown was accomplished.

Figure 14 shows records of a landing, a take-off, and a slow-speed static run of the aircraft over the deflectometer. These records are typical of all those taken. The only variations from one run to another were slight changes in amplitude, which are as likely due to different tracks by the deflectometer as to variations in speed or flap-setting.

The difference between the Hopedale and the Garrison landing records is due largely to plane speed. At Hopedale the C-47's slowed fairly rapidly on landing, and by the time they reached the deflectometer, their speed would be less than c_{min}, while at Garrison the speed of the C-131 was greater than c_{min} even as it passed the measuring point. In other words, the wave recorded at Garrison is almost completely a "forced" wave.

On all three take-offs the plane started its run about 1700 ft from the deflectometer and was in the air by about 500 ft beyond. All the take-off records show the odd "double" characteristic of the one shown in Fig. 14. The second wave cannot be a reflection from the shore as it arrives much too early. The most logical explanation is as follows: As the plane starts its take-off run, it gains speed rapidly and passes through c_{min}, generating a large wave which then falls behind the forced wave that accompanies the plane. Taking velocity information from Fig. 11, which is roughly applicable, the time separation of the first and second waves is of the right order. The slower C-47's at Hopedale produced a long following train rather than a discrete wave.

The "static" deflection due to the C-131's taxiing over the deflectometer had an amplitude of about 0.6 in., which compares with deflections measured by the SIPRE group of from 0.7 to 1.5 in., depending on how long the plane sat at their measuring point. The calibration of the deflectometer was uncertain by at least 20% due to low battery voltage in the cold weather.

HIGH-FREQUENCY AND AIR-COUPLED WAVES, GARRISON DAM

At Garrison Dam during the tests reported above, a number of seismic tests were carried out under the direction of Mr. Donald H. Clements of the Willow Run Laboratories of The University of Michigan.

Standard, commercial, 4-cps geophones were used and the recording was done wide-band on magnetic tape. The usual source was a 110-lb cylindrical weight dropped onto the ice from a height of several feet. Continuous trains of flexural waves in the frequency range of from 5 to 120 cps were observed. Figure 15 shows one of the records obtained by recording from the magnetic tape onto a standard recording camera. Some filtering of the frequencies above 60 cps has been done to improve the record quality.

Figure 16 shows flexural wave dispersion data obtained from the record shown in Fig. 15. The calculated curve shown on Fig. 16 has been calculated from the known water depth of 2500 cm and ice thickness of 60 cm and an assumed value of γ of 833 cm. The value of γ is somewhat low in comparison with the value of 1000 cm deduced from resonance measurements on identical ice at Mille Lacs. However, variations in water depth and other factors may be responsible for the difference.

No good air-coupled waves were observed from the weight drops. Their frequency for this ice should be about 85 cps and some questionable observations were obtained by firing a shotgun directly at the ice from a height of a few feet.

REFERENCES

1. Greenhill, A. G., "Wave Motion in Hydrodynamics," Am. J. Math., 9, 62-112 (1887).

2. Ewing, M., and Crary, A. P., "Propagation of Elastic Waves in Ice, II," Physics, 5, 181-184 (1934).

3. Press, F., and Ewing, M., "Propagation of Elastic Waves in a Floating Ice Sheet," Trans. A.G.U., 32, 673-678 (1951).

4. Wilson, James T., Coupling between Moving Loads and Flexural Waves in Floating Ice Sheets, SIPRE Report 34, 1955.

5. Assur, A., Airfields on Floating Ice Sheets, SIPRE Report 36, Prelim. Ed., 1956.

6. Herz, H., Gesammelte Werke, Barth, Leipzig, 1885, pp. 288-294.

7. Lamb, H., "On Waves due to a Travelling Disturbance," Phil. Mag. Sixth Ses., 31, 386-399 (1916).

8. Kenney, J. T., Jr., "Steady-State Vibrations of Beam on Elastic Foundation for Moving Load," J. Appl. Mech., 21, 359-365 (1954).

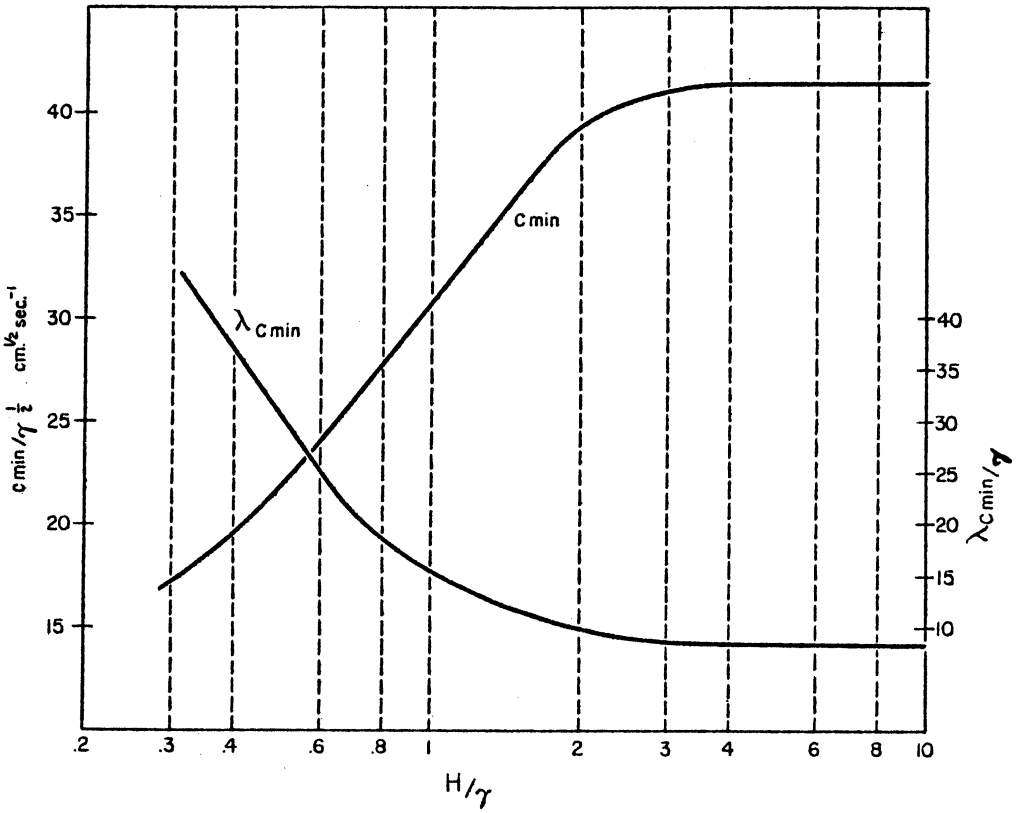

Fig. 1. Wave-velocity minimum, c_{min}, and wavelength at c_{min} as a function of H/γ.

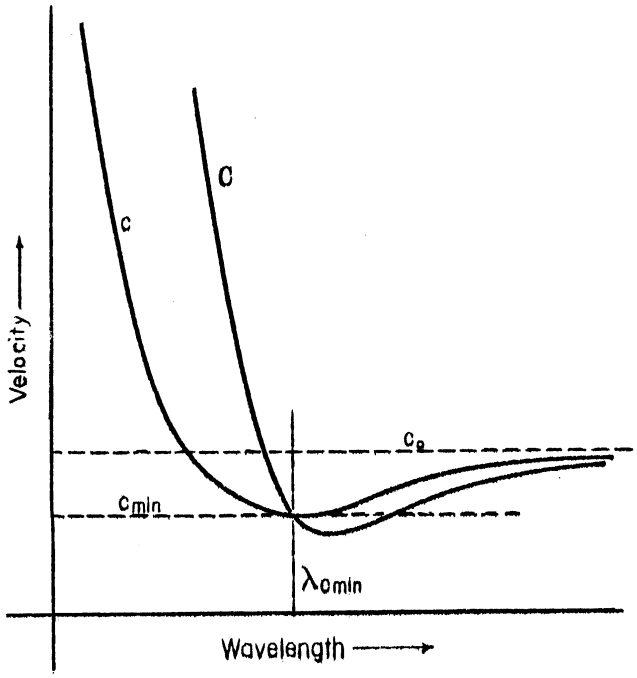

Fig. 2. Schematic plot of group and wave velocity as a function of wavelength.

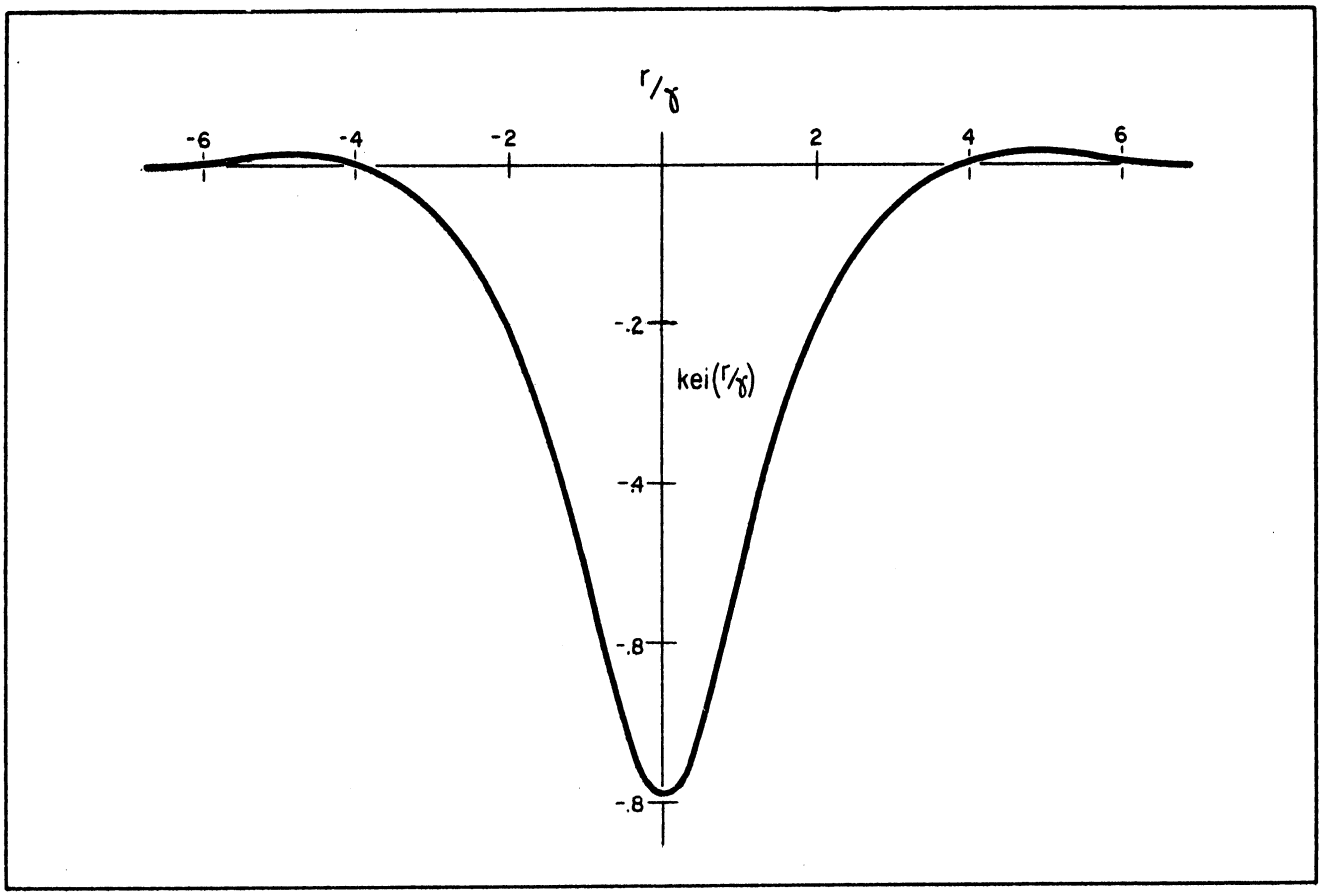

Fig. 3. kei (r/γ) as a function of r/γ.

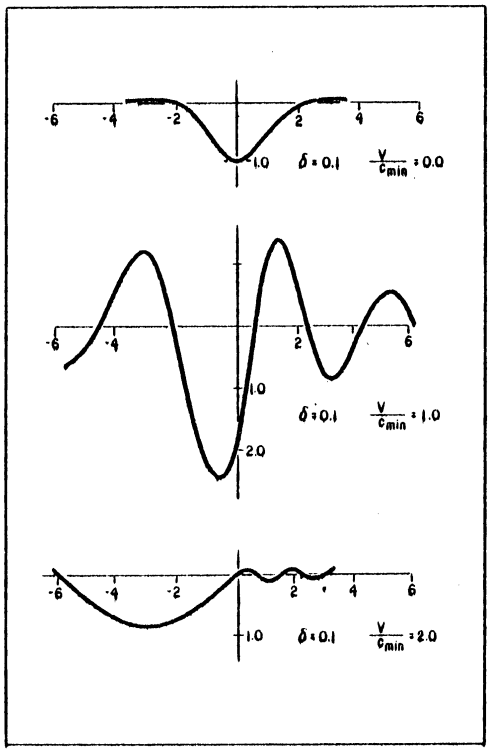

Fig. 4. Deflection curves after Kenney.[8]

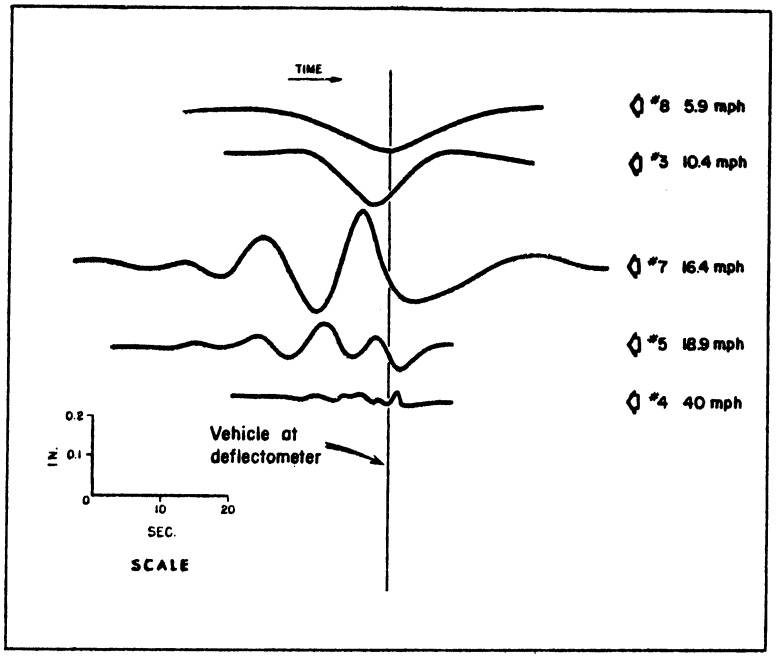

Fig. 5. Deflection records obtained at Mille Lacs, Minnesota. Weapons carried (6000 lb) traveling at constant speed. Ice 2 ft thick. Water 10 ft deep.

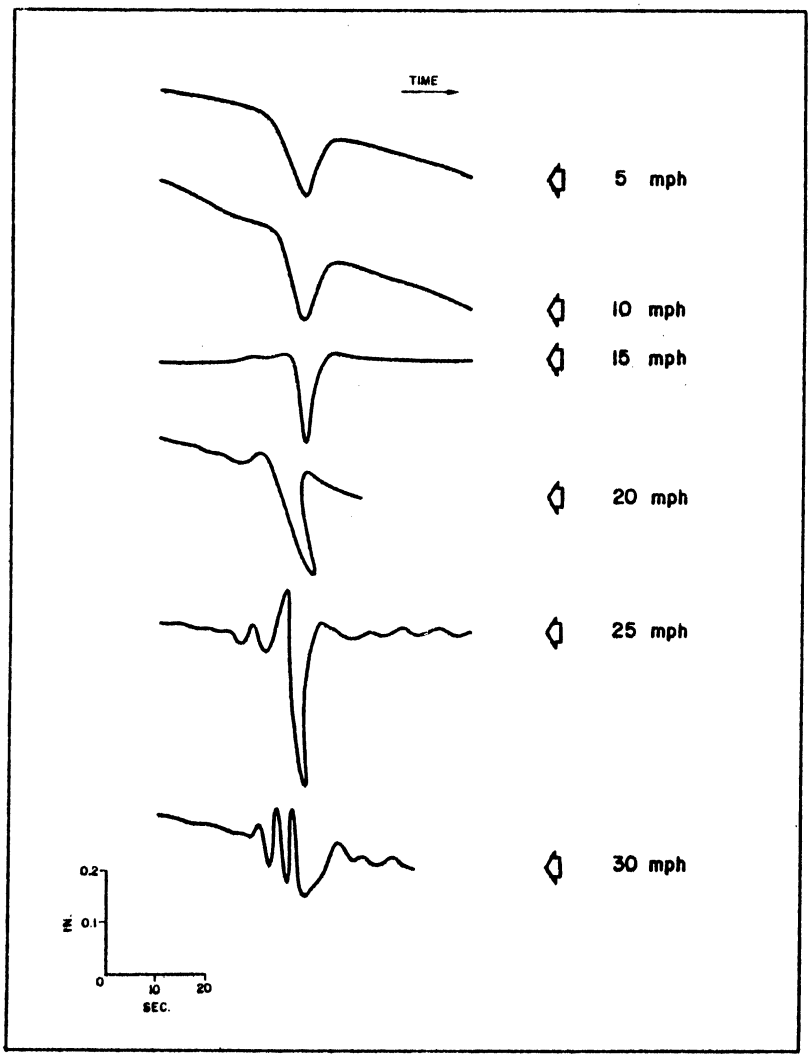

Fig. 6. Deflection records obtained at Hopedale, Labrador. Weapons carrier (6000 lb) traveling at constant speed. Ice 2+ ft thick. Water 40 ft deep.

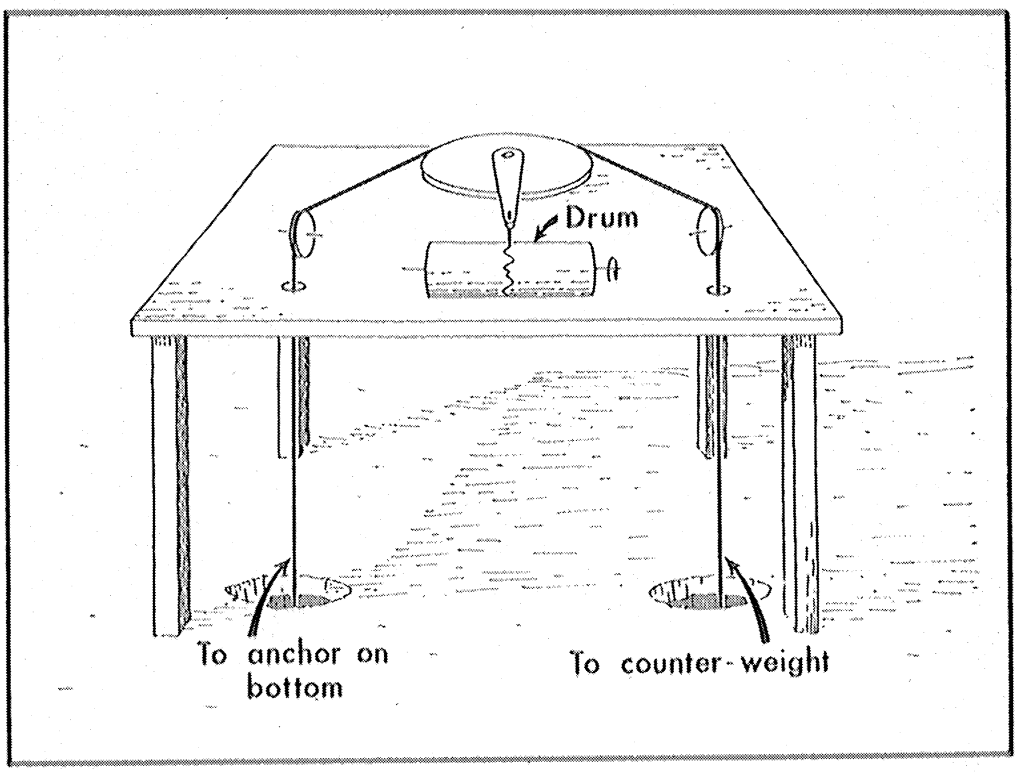

Fig. 7. Deflectometer used at Hopedale.

Fig. 8. Photograph of deflectometer used at Hopedale.

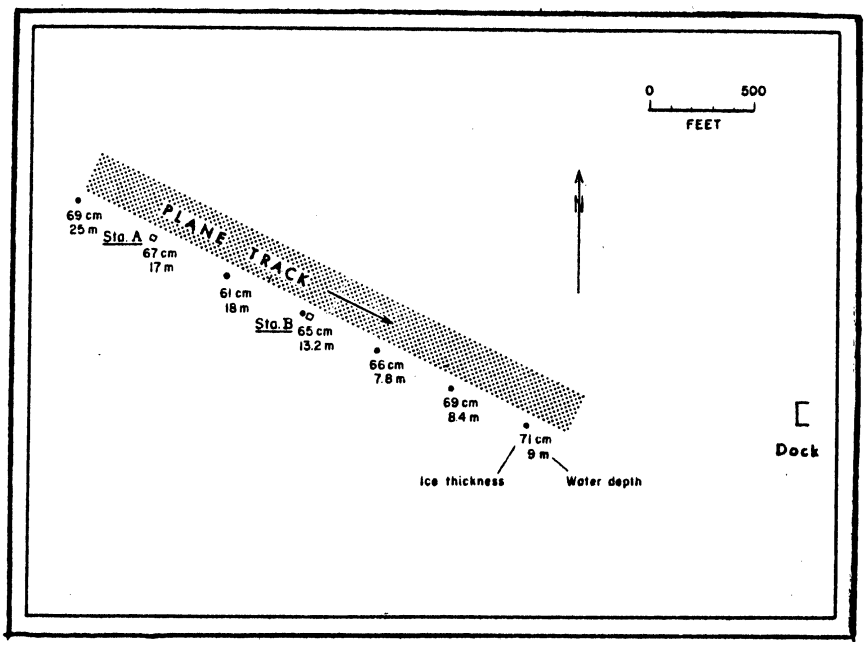

Fig. 9. Sketch map of the landing strip on the bay at Hopedale, Labrador.

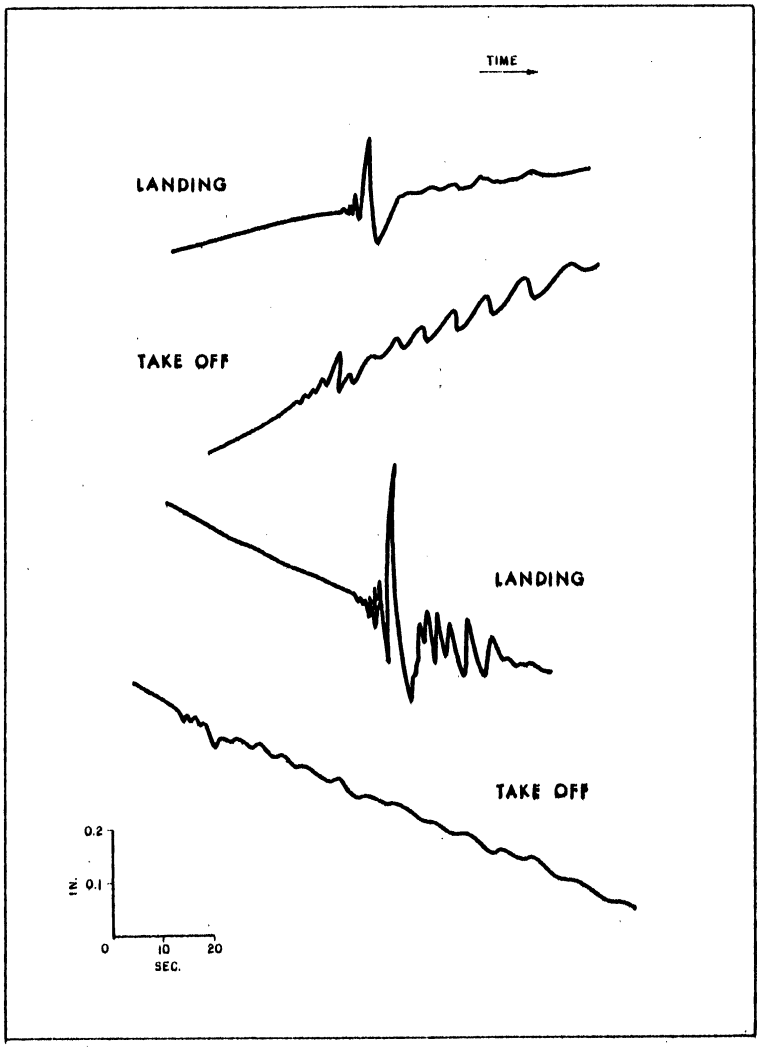

Fig. 10. Deflection records of C-47 landings and take-offs at Hopedale, Labrador.

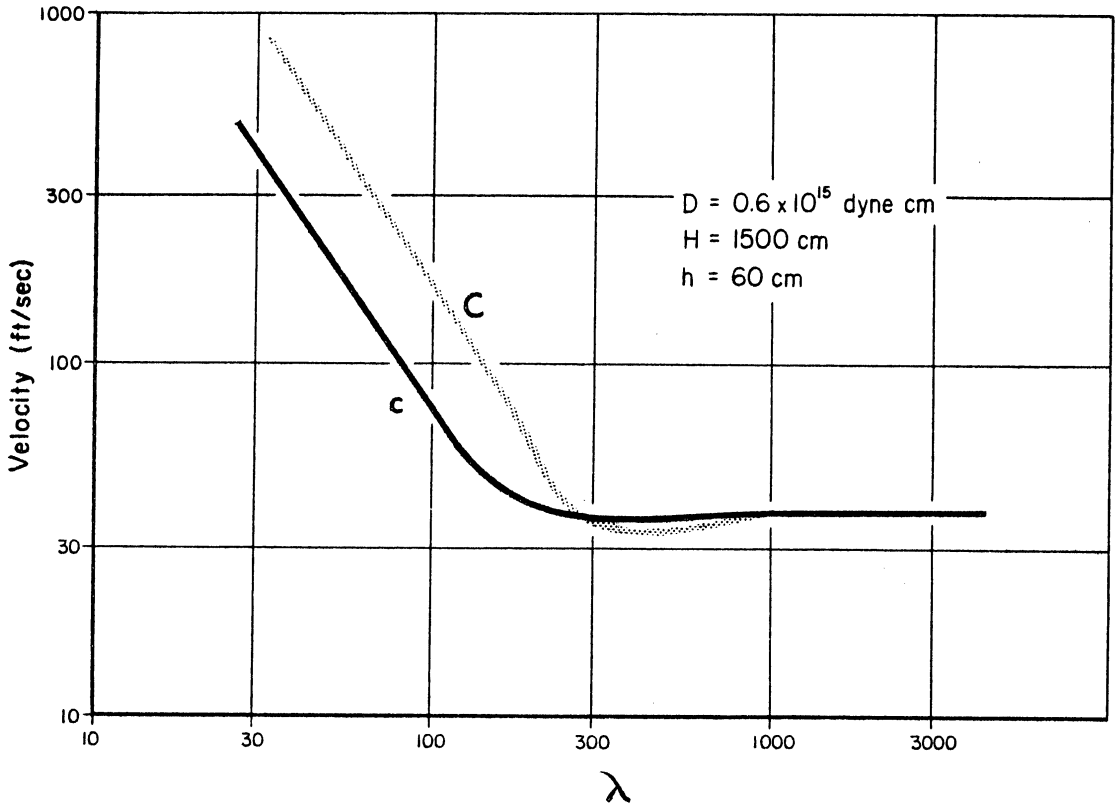

Fig. 11. Wave and group velocity as a function of wavelength.

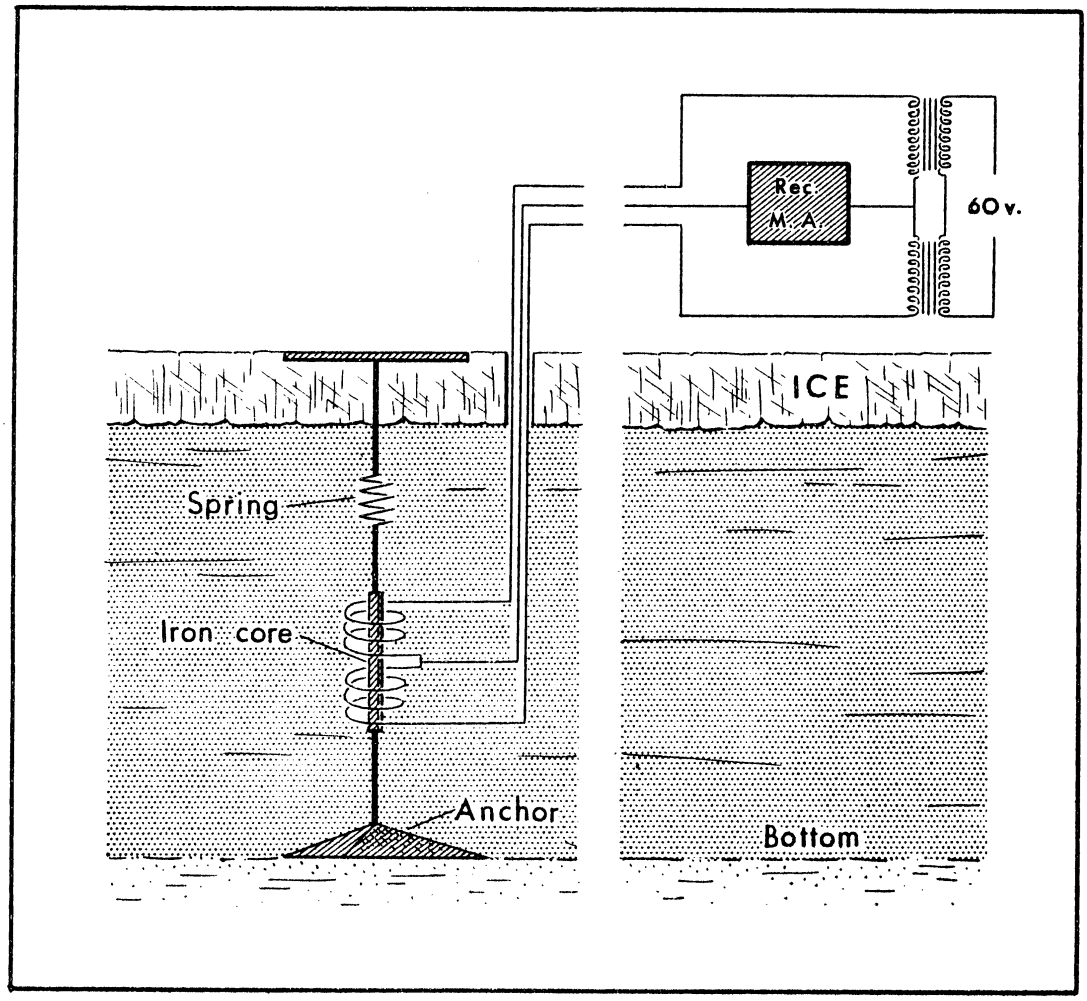

Fig. 12. Schematic drawing of the deflectometer used at Garrison, North Dakota.

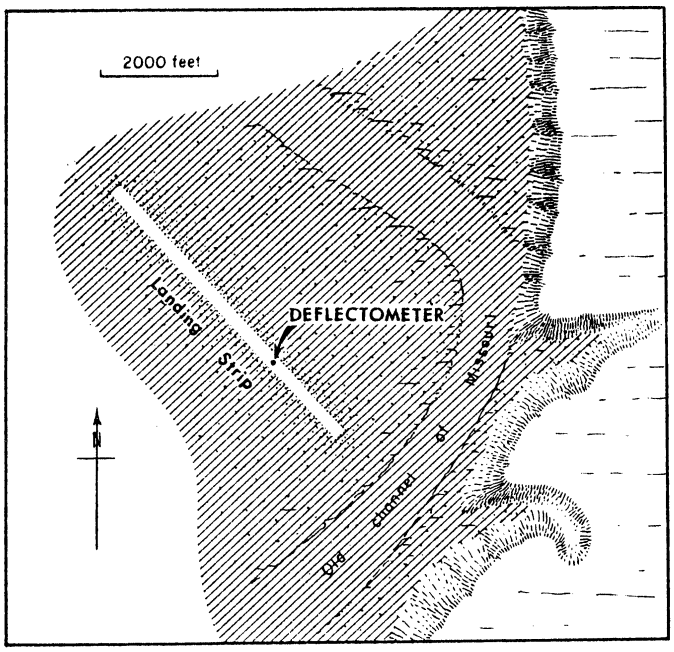

Fig. 13. Sketch map of the landing strip at Garrison, North Dakota.

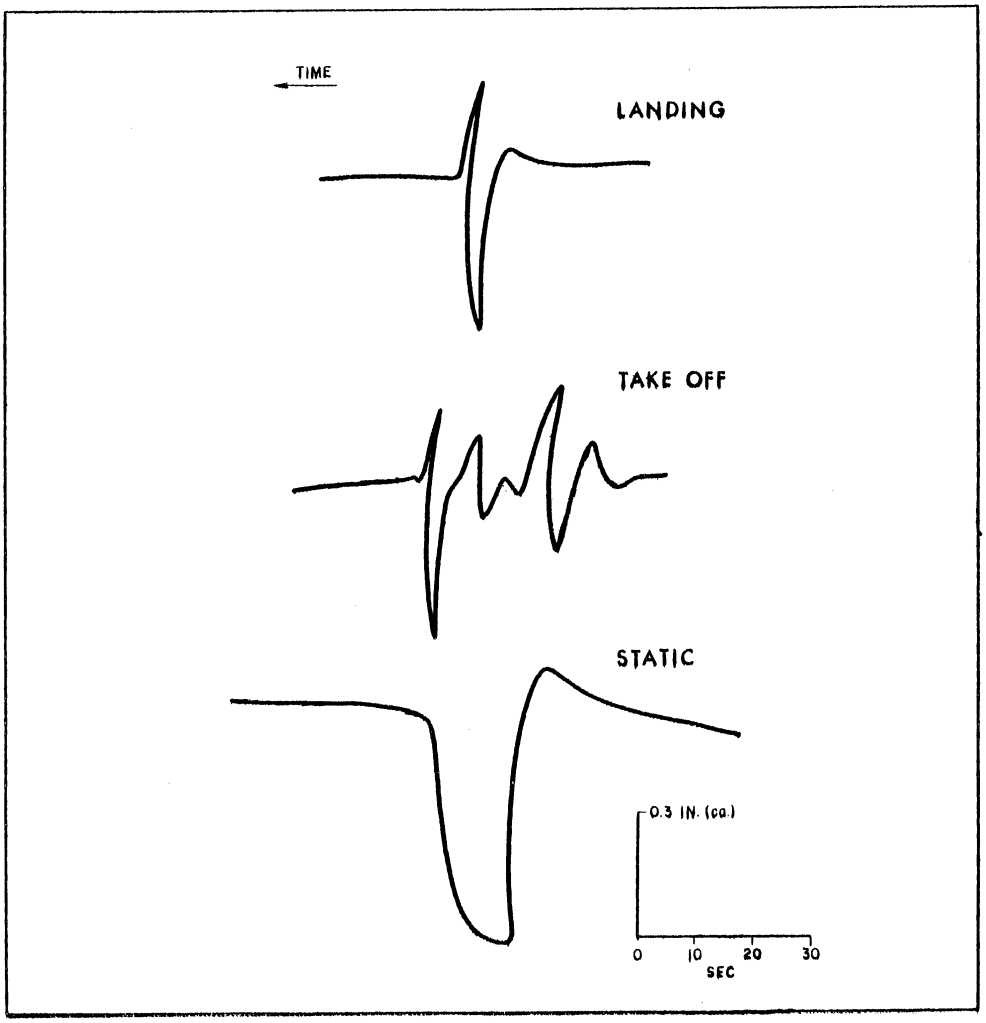

Fig. 14. Landing, take-off, and "static" records of a C-131 on the ice at Garrison, North Dakota.

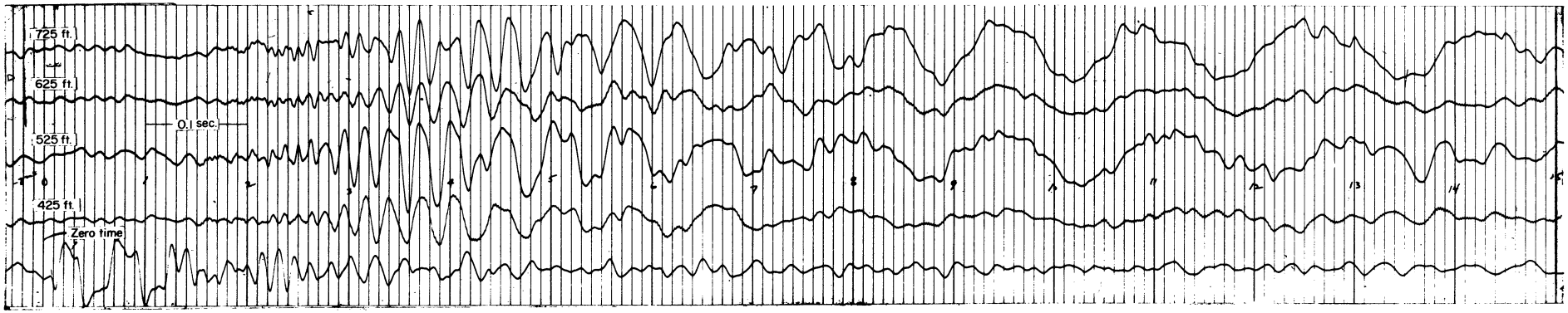

Fig. 15. Photograph of seismogram recorded at Garrison, North Dakota. Ice thickness 2 ft, water depth 83 ft.

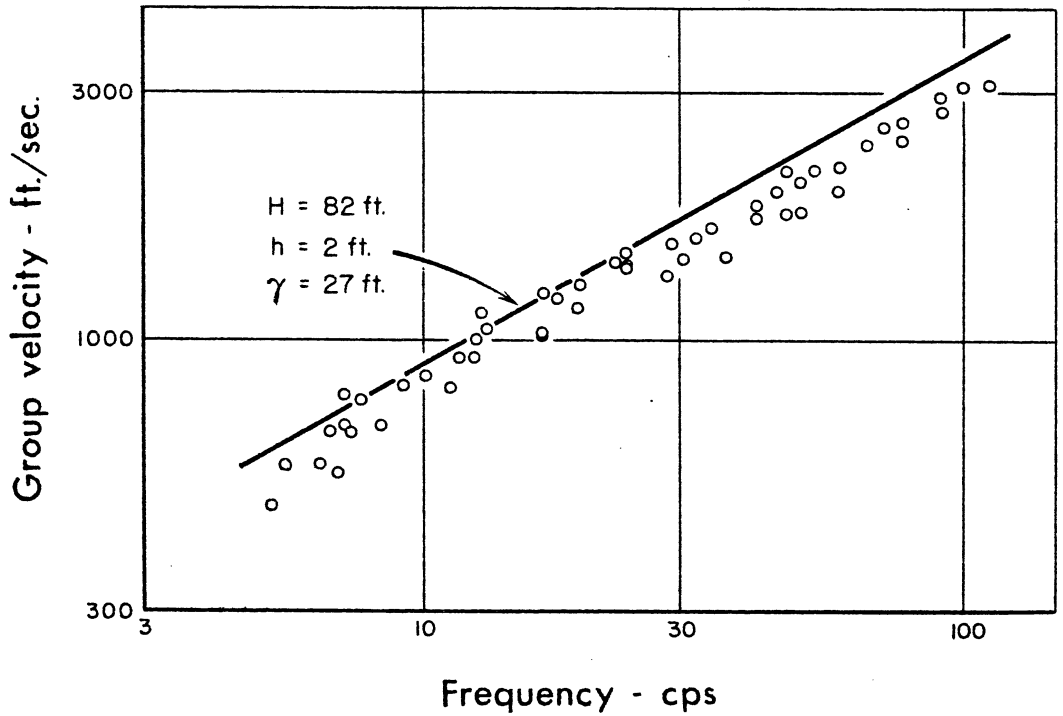

Fig. 16. Observed dispersion, Garrison, North Dakota.